Orientation imaging microscopic observations of in situ deformed ultra low carbon steel

Balke, P.; de Hosson, J.T.M.

Published in:
Scripta Materialia

DOI:
10.1016/S1359-6462(00)00632-1

Publication date:
2001

PERGAMON

Scripta mater. 44 (2001) 461–466

Scripta MATERIALIA

www.elsevier.com/locate/scriptamat

ORIENTATION IMAGING MICROSCOPIC OBSERVATIONS OF IN SITU DEFORMED ULTRA LOW CARBON STEEL

P. Balke and J.Th.M. De Hosson

Department of Applied, Materials Science Center and Netherlands Institute for Metals Research, University of Groningen, Nijenborgh 4, 9747 AG Groningen, The Netherlands

(Received April 3, 2000)
(Accepted in revised form September 13, 2000)

Keywords: Steel; Scanning electron microscope; Electron diffraction; Plasticity; Texture

1. Introduction

The major applications for Ultra Low Carbon (ULC) steel sheets can be found in the car industry for its excellent drawability characteristics. The drawability of a sheet material is defined as the degree of plastic flow in the plane of the sheet [1]. It is well known that this increases with the development of the {111} texture. Other texture components, such as the {001}, have been found to be detrimental [1,2]. Hutchinson [3] has recently reviewed the relationship between steel making practice and mechanical anisotropy. He made the point that high purity steels offer the best thinning resistance as measured by r-value (i.e. the ratio between the width strain ϵ_w (in the sheet plane at 90° to the tensile axis) to the through-thickness strain, ϵ_t. These observations are usually correlated with the strong $<111>$ fiber texture that can be based on arguments from crystal plasticity [4].

The physical properties of ULC steel sheet have been extensively studied, particularly in correlation to its texture. However, only scant information is available of the microstructural evolution during deformation. This paper concentrates on a detailed examination of the dynamics of the microstructure.

We performed in-situ SEM tensile experiments on ULC steel sheet. The purpose was to observe the response of the different textured grains on tensile loading and to quantify the lattice rotation of the crystals. A distinction was made between regular and irregular rotations, the slip system activity was monitored and quantified and the evolution of the substructure was analysed. A combination of Scanning Electron Microscopy (Philips-FEG-XL30S SEM) with an Electron Backscatter Diffraction system (EBSD), Transmission Electron Microscopy (TEM) and in-situ tensile tests in an Environmental Scanning Electron Microscope (Philips-FEG-XL30 ESEM) has been utilised.

2. Experimental

Tensile experiments were carried out inside a Philips ESEM XL30–FEG on non-stabilised Ultra Low Carbon (ULC) Steel. The anisotropic behaviour in the Reference Direction (RD)–Transverse Direction (TD) plane was studied making use of two types of tensile samples: 1) parallel to the RD with the TD in plane and 2) parallel to the TD with RD in plane. The elongation rate was 5 μm s^{-1} which corresponds to a deformation rate of about 2.5 10^{-4} s^{-1}. The stress-strain curves (Fig. 1) show the elastic and plastic behaviour of this material on a macroscopic scale. The yield stresses are approxi-

PII: S1359-6462(00)00632-1

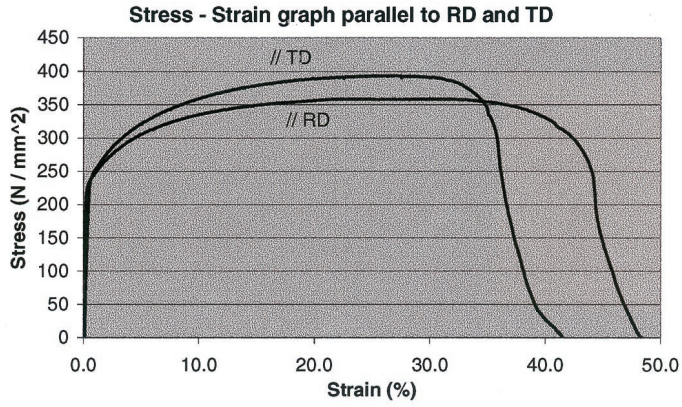

Figure 1. Stress–strain graph of ULC steel in RD and TD direction.

mately the same (250 MPa), the strains at failure for TD and RD are respectively 0.42 and 0.49, the Ultimate Tensile Strength is for TD 390 MPa and for RD 360 MPa.

Orientation Imaging Microscopy was used to obtain information about the texture in correlation to the microstructure. The measurements were performed at half the thickness of the sample in the RD-TD plane. Typically this material presents a Normal Direction (ND) or γ-fibre texture along $<111>$//ND, which can be seen in Fig. 2. Cold rolled sheet forming enhances the RD or α-fibre texture along $<011>$//RD, after recrystallization this results in a minor texture component in ULC steel. The grain size ranges between 5 and 35 μm, the average grain size being 22 μm and 18 μm if low angle boundaries are included.

During the in-situ tensile tests the microstructural evolution was monitored. In addition at 0, 10, 20 and 30% macroscopic strain, orientation measurements were performed with an EBSD system operating at 15 kV. The successive ordering of the orientations (rotations) of some grains was monitored. Those kind of measurements are very sensitive to the alignment of the sample, therefore several indents were placed on the sample to function as a reference frame.

The information about the amount of stored energy during deformation can only be studied by topographic changes in an (E)SEM. Surface roughening occurred by formation of slip lines or slip bands. It provides information about the deformation properties of different textured grains. However, the dislocation density or dislocation configuration can not be observed directly with surface micros-

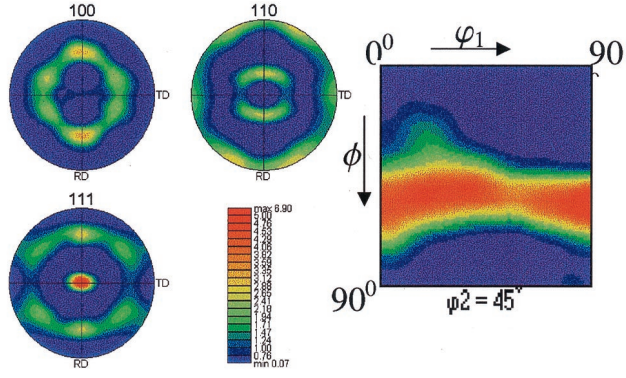

Figure 2. Pole figures and respectively the orientation distribution function representing the ULC steel texture.

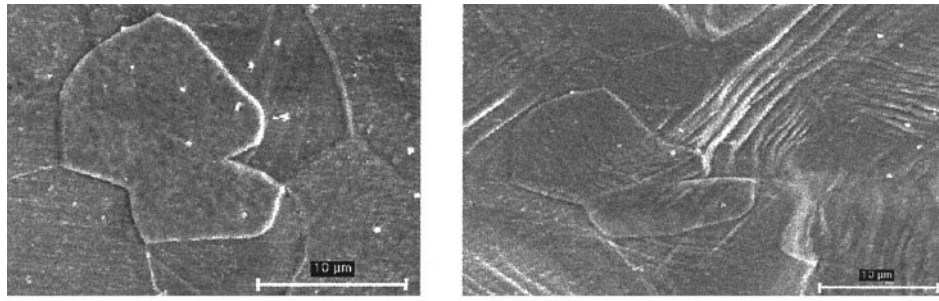

Figure 3. a: Microstructure at 3.3% strain; b: microstructure at 40% strain.

copy. The dislocation networks, which often appear as subcell boundaries in a deformed grain were observed with a JEOL 200 CX TEM operating at 200 kV.

3. Results

In general ULC steel shows a typical microstructure after etching with 2% Nital. Two types of grains can be observed, "raised" and "surface" grains. The surface grains, which have a higher etching rate relative to the raised grains, remain flat at the surface where the raised grains with a relatively lower etching rate cause topographical differences. The surface grains show a strong tendency toward a <111> texture whereas the raised grains have strong tendency toward a <001> texture. Consequently, the preferential etching of these grains is due to differences in crystallographic orientation [1].

When the stress locally exceeds the critical resolved shear stress a certain slip system is activated. Typical slip systems for BCC materials are the {011} or {112} planes in the <111> directions. The activated systems will produce slip lines on the sample surface. Our microstructural observations showed that first in the <111> textured grains the slip systems were activated i.e. slip lines were exposed (Fig. 3a). Further straining of the sample resulted in slip bands in the <111> textured grains and some <001> textured grains showed slip lines. The characteristic response of the <001> grains on loading the sample is a low slip activity and slight rotation due to the constraint of the surrounding grains (Fig. 3b). The observed microstructural response on loading in direction 1) and direction 2) showed also significant differences in the activity of slip systems. The amount of slip bands/lines for samples loaded in longitudinal direction 1 (//RD) were higher than for samples loaded in transverse direction 2 (//TD).

A TEM image of the deformed ULC Steel sheet is shown in Fig. 4. It can be seen that the deformation intensifies near the grain boundaries and triple junctions due to the constraint from the surrounding grains. In the centre of the grain interior there are long elongated subcells.

The rotation during tensile testing was observed and quantified for fourty grains. The series in direction 2 were performed until 30% macroscopic strain. The quantification of the rotation was observed for both the <001> textured grains as well as for the <111> textured grains. There were no differences in rotation axes between the different textured grains, the rotation axes were all between <001> and <012>. The rotation angles for the surface grains were slightly higher than for the raised grains, yet the deviation was also higher (see Table 1).

The successive rotation of some grains in the interior of ULC Steel (Fig. 5) was visualised. The orientations are shown in Fig. 6. Two <001> pole figures are presented, one of a <111> textured grain (Fig. 6a) and one of a <001> textured grain (Fig 6a). The points of the <111> textured grains

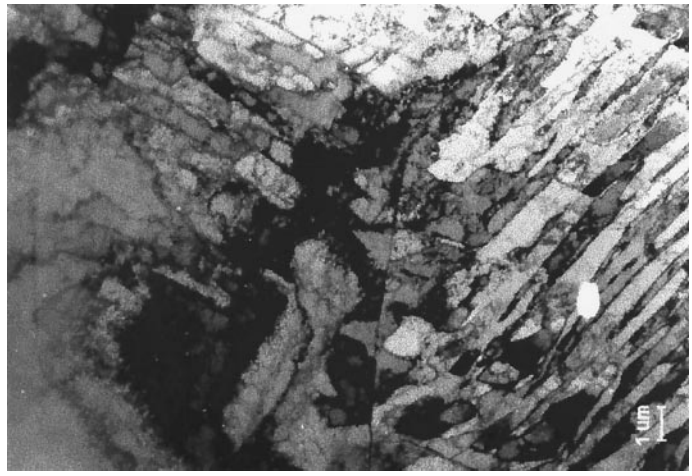

Figure 4. TEM image of 30% strained ULC steel showing a triple junction.

were all successive and within the error induced by the formation of subcells. The <001> textured grain, however, did not show a successive tendency in the ordering of its orientation points.

4. Discussion

It has been demonstrated that the plasticity of ULC steel is enhanced when a high proportion of grains is oriented with their <111> directions parallel to the surface normal. Other texture components, such as the <001>, have been found to be detrimental. In other words, the plasticity of the <111> textured grain is relatively higher then the <001> textured grains in the RD-TD plane [4]. Our microstructural observations during tensile testing confirmed the relatively higher plasticity of the <111> textured grains.

The anisotropy in the RD-TD plane was demonstrated by two tensile tests with the tensile axis parallel and perpendicular to the RD. The result was a difference in the amount of slip lines/bands. The anisotropic behaviour of the material in the RD-TD plane is obvious from our texture measurements, which still showed a clear rolling texture. The <011> texture (one of the slip planes) is symmetrically 30° off in the RD–ND plane. This explains the higher amount of slip lines parallel to the RD axis.

The regular lattice rotations, as observed in grain 166 (Fig. 6b), are simply caused by the constraint of the surrounding grains and the slip system activity, this behaviour is according to the theory of polycrystal plasticity [5]. The different values for the average rotation angles for the different textures can be explained by the fact that, the rate of change of the orientation of any particular grain is proportional to the current rate of slip on the active slip system(s) [6]. The large errors are caused by the presence of relatively stable orientated grains.

TABLE 1
Quantification of Rotation Angle at 30% Strain

Rotation Axis	Rotation angle (°)
<001>	7 ± 2
<111>	8 ± 3

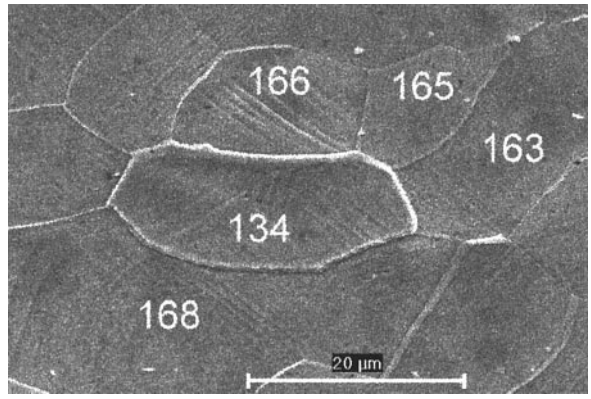

Figure 5. SEM image of grain configuration used for rotation analyses.

Irregular lattice rotations occurred in some cases, for instance in grain 134 (Fig. 6a). In this specific case the irregular behaviour occurred between 10% and 20% strain. It is likely that in this interval an additional slip system becomes active. This slip system can be seen in the SEM image (Fig. 5).

The stable texture components for tensile testing are the {001}<110> and {111}<110> components according to Schouwenaars et al [7]. Our observations showed indeed the tendency of rotation to the stable {111}<110> component for the almost {111}<110> textured grains. The rotation of the <001>{001} textured is not sufficient to deduce a trend to one of those stable configurations.

TEM studies were performed on the interior of the deformed grains. It showed that near the grain boundaries the deformation intensifies. The deformation in the centre of the grain is organised in subcells. The elongated directions of the subcells in one grain relative to the other are perpendicular like the slip lines in the SEM images. If we compare the distances between sliplines and subcell boundaries they are more or less the same; i.e. *1 µm* which is typical for slip line inter distances. Therefore, we may conclude that the long subcell boundaries correspond to the slip lines which can be seen in the SEM images.

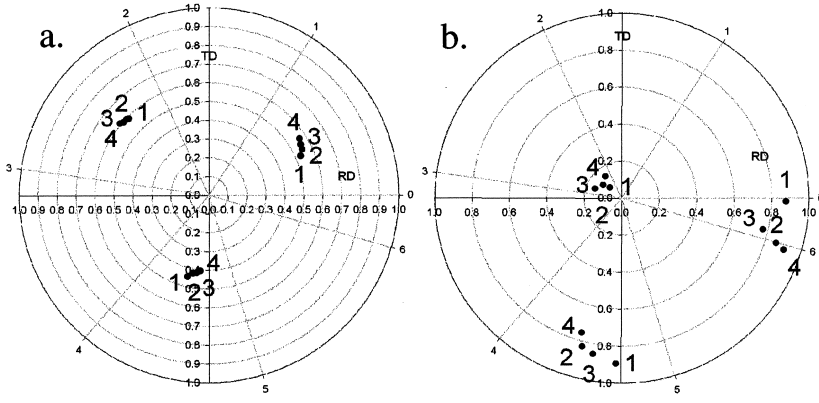

Figure 6. Successive orientations in <001> Pole figures for a) grain 166 and b) grain 134.

5. Summary

In this paper the microscopic behaviour during in situ tensile experiments was correlated to the macroscopic response of ULC steel sheet. The plastic flow in the plane of the sheet was highest in the RD direction, due to the presence of a rolling texture. The observed response of the different textures was quantified by the average crystal rotation. The rotation was over a <001> to <012> axis with an angle of $(7 \pm 2)^0$ for the <001> textured and $(8 \pm 3)^0$ for the <111> textured grains. Irregular crystal rotations could be explained by the fact that additional slip systems were activated during straining. The long subcell boundaries observed by TEM were linked to the slip lines which were observed in the SEM.

Acknowledgments

Financial support by the Netherlands Institute for Metals Research is gratefully acknowledged.

References

1. R. K. Ray, Int. Mater. Rev. 39(4), 129 (1994).
2. M. Caul, Mater. Characterisation 38, 155 (1997).
3. W. B. Hutchinson, in Textures of Materials ICOTOM-10, ed. H. J. Bunge, p. 917, Trans Tech Publishers, Zurich, Switzerland (1994).
4. U. F. Kocks, C. N. Tomé, and H.-R. Wenk, Texture and Anisotropy, p. 390, Cambridge University Press, Cambridge, UK (1998).
5. N. Y. Zolotorevsky, Scripta Mater. 38(8), 1263 (1998).
6. T. Takeshita, in 8th International Conference on Textures and Materials, ed. J. S. Kallend and G. Gottstein, pp. 445–448 (1988).
7. R. Schouwenaars, ISIJ Int. 34(4), 366 (1994).